Delineation of Two Functionally Distinct γ_{PDE} Binding Sites on the Bovine Retinal cGMP Phosphodiesterase by a Mutant γ_{PDE} Subunit†

Allan L. Berger, Richard A. Cerione,* and Jon W. Erickson

College of Veterinary Medicine, Department of Molecular Medicine, Cornell University, Ithaca, New York 14853

Received July 13, 1998; Revised Manuscript Received October 15, 1998

ABSTRACT: The γ subunit of the retinal cGMP phosphodiesterase (γ_{PDE}) acts as an inhibitor of phosphodiesterase (PDE) catalytic activity and mediates enzyme regulation by the α subunit of the GTP-binding protein transducin (α_T). In this work, we describe a full length, doubly point-mutated γ subunit, C68S, Y84C γ_{PDE}, which binds to PDE with increased affinity but has a decreased ability to inhibit the enzyme. Fluorescence studies monitoring the competition between wild-type γ_{PDE} and the C68S, Y84C γPDE mutant suggest that the mutant γ_{PDE} binds with high affinity to only half of the total sites occupied by wild-type γ_{PDE}. Competition studies between wild-type γ_{PDE} and the mutant further suggest that the wild-type protein is able to fully inhibit PDE activity even when the mutant γ_{PDE} occupies its high-affinity binding site on PDE. Taken together, our findings are consistent with a model in which there are two distinguishable binding sites for γ_{PDE} on the PDE enzyme but that only one of the two sites mediates PDE inhibition.

The retinal cGMP phosphodiesterase (PDE)[1] serves a critical role in the vertebrate phototransduction system by converting a biochemical cascade of protein−protein interactions into a change in second messenger (cGMP) concentrations (see refs *1* and *2*). This signaling system has served as a paradigm for understanding how seven-membrane-spanning receptors couple to heterotrimeric GTP-binding proteins and how activated G proteins regulate the activities of their biological effectors. The receptor in this signal transduction pathway, rhodopsin (made up of the protein backbone opsin and the chromophore retinal), initiates the signaling pathway following the absorption of light. This leads to the formation of a complex between rhodopsin and the G protein transducin (which consists of a 39 kDa α subunit, designated α_T, a 35 kDa β subunit, and an ∼8 kDa γ subunit, designated γ_T). Within this complex, rhodopsin stimulates the exchange of GDP for GTP that in turn causes the dissociation of transducin into an α_TGTP species and intact $\beta\gamma_T$ complex. The α_TGTP then stimulates the biological effector, the cyclic GMP phosphodiesterase, a tetrameric enzyme consisting of two larger subunits (designated α_{PDE} and β_{PDE}, $M_r \sim 85$ kDa) and two identical smaller subunits designated γ_{PDE} ($M_r \sim 14$ kDa; *3*). The γ_{PDE} subunits serve as the binding sites for the GTP-bound α_T subunit (*4*, *5*). The stimulation of enzyme activity continues until the GTP bound to α_T is hydrolyzed to GDP; thus, the GTPase activity of α_T returns the signaling system to its starting point.

The γ_{PDE} subunits have been shown to bind and regulate the PDE through multiple binding sites. There is a central cationic region of γ_{PDE} which appears to be responsible for the binding affinity of γ_{PDE} for α,β_{PDE} (*6*, *7*) and a carboxyl terminal domain which inhibits the activity of α,β_{PDE} (*8*, *9*). Recently, these interactions were further defined by cross-linking studies which showed that the central cationic region of γ_{PDE} interacts with α_{PDE} 461−533 (*10*), and that the carboxyl terminal domain of γ_{PDE} binds to α_{PDE} 751−763 (*11*). More recently, Granovsky et al. (*12*) have suggested that the γ_{PDE} subunit inhibits the PDE enzyme by directly competing with cGMP at the active site. Other regulatory mechanisms have been described for the PDE in addition to the direct interaction between the γ_{PDE} subunits and the larger (catalytic) subunits. Each catalytic subunit has both a catalytic and a noncatalytic cGMP binding site (*13*, *14*), and the occupation of the noncatalytic cGMP binding sites by cGMP has been shown to influence the association of γ_{PDE} with the catalytic subunits (*15*, *16*). An additional level of regulatory complexity involves the binding of α_TGTP to PDE. For example, Phillips et al. (*17*) demonstrated that when two α_TGTPγS molecules were simultaneously presented to the PDE by a bivalent anti-α_T antibody, the cGMP hydrolysis response was potentiated relative to the catalytic activity caused by the binding of single α_TGTPγS activators.

During the past several years, our laboratory has set out to develop and utilize fluorescence spectroscopic approaches to probe the mechanisms underlying the activation of the cyclic GMP PDE (*18*, *19*). In the present study, we show that a γ_{PDE} C68S, Y84C mutant binds with higher affinity to PDE compared to wild-type γ_{PDE} but the mutant is a significantly less potent inhibitor of PDE activity. The mutated γ_{PDE} protein appears to compete with high affinity for only half of the total sites occupied by the wild-type γ_{PDE} subunit, and PDE molecules that have one site occupied by the γ_{PDE} mutant can still be fully inhibited by wild type γ_{PDE}. These findings suggest that the two γ_{PDE} sites on α,β_{PDE} are

† Supported by NIH Grant EY06429. A.L.B. is a recipient of an Advanced Predoctoral Fellowship from the PhRMA Foundation.

[1] Abbreviations: PDE, retinal cGMP phosphodiesterase; tPDE, trypsin-activated PDE; IAF, 5-iodacetamidofluorescein; NEM, *N*-ethylmaleimide; F-WT γ_{PDE}, IAF-labeled wild-type γ_{PDE}; F-C68S, Y84C γ_{PDE}, IAF-labeled C68S, Y84C mutant γ_{PDE}; NEM-C68S, Y84C γ_{PDE}, NEM-labeled C68S, Y84C γ_{PDE}, α_T, transducin α subunit.

10.1021/bi981683m CCC: $18.00 © 1999 American Chemical Society
Published on Web 12/31/1998

not identical and that only one of the two sites is catalytically active.

EXPERIMENTAL PROCEDURES

Materials. SP-Sepharose and Phenyl Sepharose were obtained from Pharmacia (Piscataway, NJ). Factor Xa was purchased from New England Biolabs (Beverly, MA). 5-Iodoacetamidofluorescein was purchased from Molecular Probes, Inc. (Eugene, OR). Dark-adapted bovine retina were purchased from Hormel Meat Packers (Austin, MN). All other chemicals and enzymes were purchased from Sigma Chemical Co. (St. Louis, MO). The pLCIIFXSG plasmid was a gift from Dr. Heidi Hamm (Northwestern University School of Medicine).

γ_{PDE} Expression and Purification. The synthetic γ_{PDE} cDNA was subcloned from the pLcIIFXSG vector (*20*) into the pET-21a expression vector using the restriction endonucleases BamHI and HindIII (pET-21a-SG). The γ_{PDE} double mutant C68S, Y84C was introduced into the γ_{PDE} cDNA using the polymerase chain reaction. For this reaction, two oligonucleotide probes were synthesized, one coding for the C68S mutation and with a unique KpnI restriction enzyme site just upstream of the mutation (5′-CTGGGTAC-CGACATCACCGTTATC-AGCCCATGGG-3′), and one containing the antisense codon for the Y84C (5′-AAGC-TTCTAGATGATACCGCACTGAGCCAGTTCGTGT-AGCTC-3′) mutation with a unique HindIII restriction enzyme site just upstream of the termination codon for the protein. Using these two oligonucleotides as primers for the PCR technique resulted in the amplification of an approximately 100 bp sequence containing the two mutations. The PCR product and the pET-21a-SG plasmid were each digested with KpnI and HindIII and purified by agarose gel electrophoresis. Ligation of the two DNA fragments generated an expression vector that encoded the C68S, Y84C γ_{PDE} as a fusion protein with 13 amino acids of the T7 protein at the amino terminus. The vector was sequenced by the New York State Center for Advanced Technology using the Sanger dideoxynucleotide DNA sequencing method to verify the sequence of the entire coding region of the C68S, Y84C γ_{PDE}.

The C68S, Y84C γ_{PDE} was expressed in *Escherichia coli* strain BL21(DE3) and purified as described by Skiba et al. (*21*). Briefly, bacterial cells were grown at 37 °C in a Labline fermentor and induced with 0.5 mM isopropyl-1-thio-β-D-galactopyranoside for 4 h. After expression, cells were resuspended in 50 mM Tris (pH 7.5), 50 mM NaCl, 1 mM EDTA, 1 mM DTT, 100 μM PMSF, and 10 μg/mL aprotinin and sonicated. The insoluble material was removed by centrifugation at 150 000*g* for 30 min, and the supernatant was loaded on to an SP-Sepharose cation exchange column. C68S, Y84C γ_{PDE} was eluted from the column with a linear gradient of NaCl (50−500 mM), 50 mM Tris (pH 7.5), 1 mM EDTA, and 1 mM DTT. At this point, the γ_{PDE} was >90% pure based on Coomassie blue-stained SDS polyacrylamide gel electrophoresis (SDS−PAGE). The sample was dialyzed in Spectropore 2000 Da molecular weight cutoff tubing versus 20 mM HEPES, 150 mM NaCl, 5 mM $MgCl_2$, and 0.2 mM DTT, pH 7.4, and stored in aliquots at −80 °C until use.

Recombinant wild type γ_{PDE} (WT γ_{PDE}) was expressed in *E. coli* and purified as described by Berger et al. (*22*).

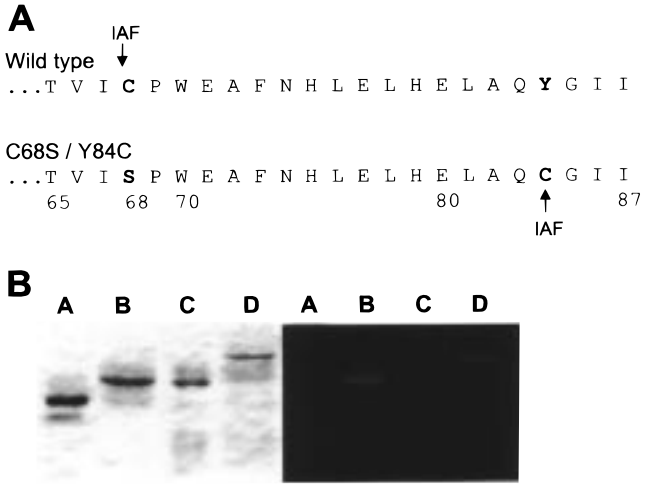

FIGURE 1: Introduction of a fluorescent reporter group near the carboxyl terminus of γ_{PDE}. Panel A shows the primary structure of F-WT γ_{PDE} and the F-C68S, Y84C mutant. Panel B shows the IAF labeling of both WT γ_{PDE} and the C68S, Y84C γ_{PDE} mutant. Labeled WT γ_{PDE} and labeled C68S, Y84C γ_{PDE} (B and D, respectively) show a retarded mobility on SDS−PAGE relative to unlabeled WT γ_{PDE} and unlabeled C68S, Y84C γ_{PDE} (A and C, respectively). Ultraviolet transillumination of the polyacrylamide gel shows that a single protein band is labeled and that band aligns with the major band in lanes B and D.

Modification of C68S, Y84C γ_{PDE} and WT γ_{PDE} with Cysteine-Reactive Compounds. γ_{PDE} species at ~5 μM concentration were reacted with 1 mM IAF at pH 7.4 for 1 h. The reaction was quenched with the addition of 30 mM DTT, and the labeled protein was separated from free probe by SDS−PAGE. Labeled protein was visualized in the gel using UV transillumination and excised (*4*, *18*). The gel slice containing the labeled γ_{PDE} was incubated in 4 volumes of distilled water at 4 °C overnight. The concentration of labeled γ_{PDE} was determined by absorbance at 490 nm, using a molar extinction coefficient of 82 000 M^{-1} cm^{-1} (*23*). NEM-labeled C68S, Y84C γ_{PDE} was similarly prepared by reacting 5 μM C68S, Y84C γ_{PDE} with 1 mM *N*-ethylmaleimide at pH 7.4 for 1 h.

Purification of Retinal PDE. Purification of holo-PDE from bovine retina was performed as previously described (*24*). Rod outer segments were purified as described by Gierschik et al. (*25*) and washed several times with isotonic buffer (10 mM HEPES, 5 mM $MgCl_2$, 1 mM DTT, 0.1 mM EDTA, 100 mM NaCl, 0.3 mM phenylmethylsulfonyl fluoride, pH 7.5). The rod outer cell membranes were then resuspended in hypotonic buffer (10 mM HEPES, 1 mM DTT, 0.1 mM EDTA, 0.3 mM PMSF, pH 7.5) to release PDE from the membranes and centrifuged at 39 000*g*. The supernatant from the hypotonic wash (containing the holo-PDE) was concentrated using an Amicon 30 000 Da molecular weight cutoff membrane.

Concentrations for proteins were determined using the Cu^{2+}/bicinchoninic acid assay (BCA protein reagent; Pierce, Rockford, IL).

Assay of PDE Inhibitory Activity. Trypsin-activated PDE (tPDE) was prepared by limited tryptic digestion of purified PDE (*24*). Trypsin at 65 μg/mL was added to 1 μM PDE and incubated at room temperature for 2 min. The reaction was quenched by the addition of 260 μg/mL soybean trypsin inhibitor. PDE activity was determined using a pH microelectrode (*26*), measured in 5 mM HEPES, 100 mM NaCl,

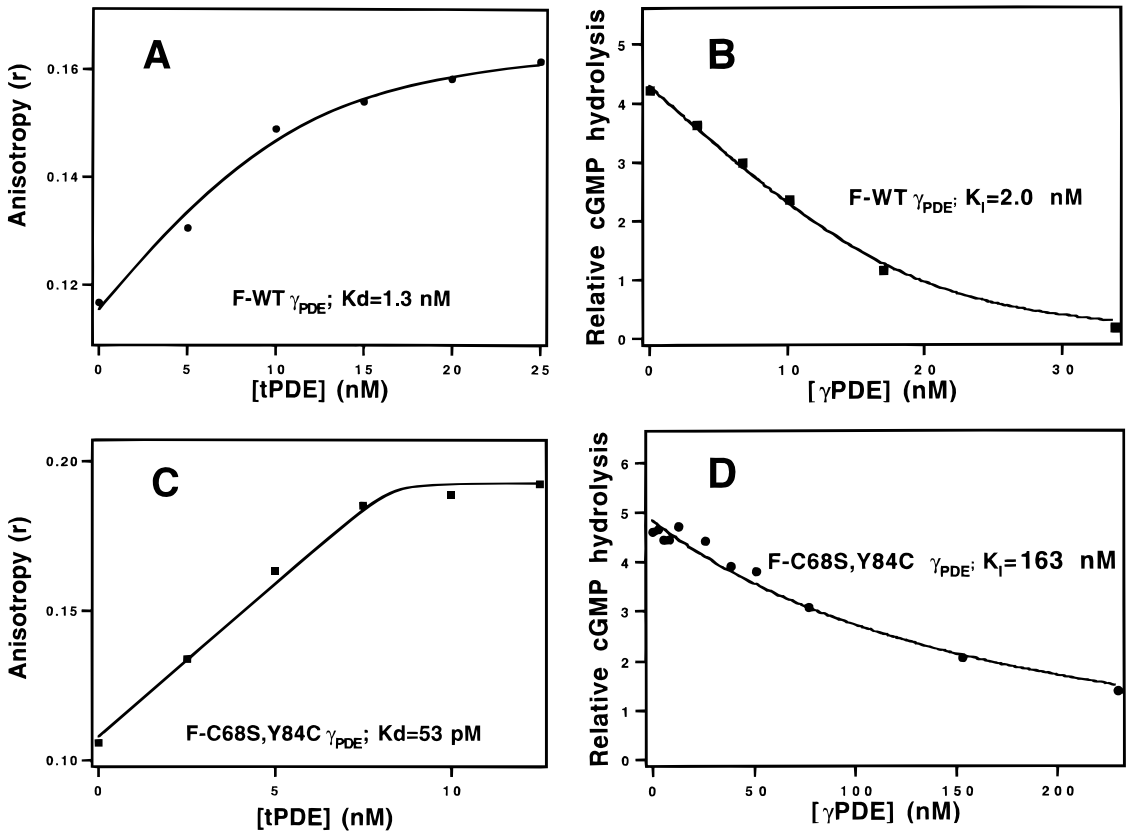

FIGURE 2: Interactions of F-WT γ_{PDE} and F-C68S, Y84C γ_{PDE} with tPDE. Panel A shows fluorescein fluorescence anisotropy of the F-WT γ_{PDE}. An 8.8 pmol (11 nM) amount of F-C68S, Y84C γ_{PDE} was bound to successive additions of 2 pmol (2.5 nM) trypsinized PDE. The curve shown is the fit to a quadratic binding equation for total tPDE binding to doubly labeled γ_{PDE}. The apparent K_D for this binding is 1.33 nM ± 0.47 nM (SE, $n = 3$). The concentration of tPDE (*x*-axis) is the concentration of α_{PDE} and β_{PDE} monomers, and the fit shows two F-WT γ_{PDE} binding sites per tPDE molecule. Panel B shows the ability of F-WT γ_{PDE} to inhibit cGMP hydrolysis. The rate of cGMP hydrolysis of 3 pmol (15 nM) of tPDE was measured using the pH microelectrode assay (see Experimental Procedures). The K_I for F-WT γ_{PDE} is 2 nM. Panel C shows fluorescein fluorescence anisotropy of the F-C68S, Y84C γ_{PDE}. A 6.6 pmol (8.3 nM) amount of F-WT γ_{PDE} was bound to successive additions of 2 pmol (2.5 nM) tPDE. The concentration of tPDE (*x*-axis) is the concentration of α,β_{PDE} dimers. The solid line fit is consistent with one F-C68S, Y84C γ_{PDE} binding site per tPDE molecule. The apparent K_D for this binding was 0.053 nM ± 0.019 (SE, $n = 3$). Panel D shows the ability of F-C68S, Y84C γ_{PDE} to inhibit cyclic GMP hydrolysis as described in panel B. The K_I for F-C68S, Y84C γ_{PDE} is 163 nM.

2 mM $MgCl_2$, and 5 mM cGMP, pH 7.5, at room temperature. Proton release from cGMP hydrolysis due to PDE activity was recorded in millivolts at one determination per second. The buffering capacity of the assay mixture was determined before and after each experiment by adding 250 nmol of KOH and recording the change in the potential of the solution. Preparations of tPDE yielding specific activities of 1500−4000 mol of cGMP/(mol of tPDE/s) were used in the experiments presented below.

Data Analysis. Anisotropy data in Figure 2 were fit to the binding equation

$$r = r_0 + r_f\left[\frac{(K_D + L_T + R_T) - \sqrt{(K_D + L_T + R_T)^2 - 4R_TL_T}}{2R_T}\right] \quad (1)$$

where r is the anisotropy value, r_0 is the initial anisotropy value, r_f is the maximum anisotropy, L_T is the total tPDE catalytic subunit concentration (i.e. the total concentration of α_{PDE} and β_{PDE} subunits) when measuring the wild-type γ_{PDE} and half of the total tPDE catalytic subunit concentration when assaying the binding of the mutant γ_{PDE} subunit, R_T is the total γ_{PDE} concentration, and K_D is the dissociation constant describing the interaction between tPDE and γ_{PDE}. In some fits a factor was used as an adjustable parameter for the concentration of tPDE in eq 1 by dividing the term L_T where it appears by n. Titrations monitoring the inhibition of PDE activity were fit to the binding equation

$$A = A_0 - (A_0 - A_f)\left[\frac{(K_I + L_T + R_T) - \sqrt{(K_I + L_T + R_T)^2 - 4R_TL_T}}{2R_T}\right] \quad (2)$$

where A is the activity, A_0 is the initial activity value, A_f is the final (inhibited) activity, L_T is the total γ_{PDE} concentration, R_T is the total tPDE concentration, and K_I is the inhibition constant. All fits were generated with IgorPro software using a least-squares fit criterion (WaveMetrics, Inc., Lake Oswego, OR).

Fluorescence Spectroscopy. Fluorescence emission anisotropy was measured on an SLM 8000C fluorimeter using a 1 × 0.3 cm quartz cuvette. The sample was diluted into 5 mM HEPES, 100 mM NaCl, and 2 mM $MgCl_2$, pH 7.5, and was stirred continuously. Excitation from a xenon lamp passed through a monochromator set at 465 nm, and orthogonal emission was monitored continuously at 520 nm.

Emission in the horizontal and vertical orientations was measured simultaneously using a monochromator set at 520 nm and a band-pass filter of 520 nm. The *G* factor was set to 1.0 by adjusting the photomultiplier tube gain prior to beginning acquisition. All measurements were made at room temperature (~22 °C).

RESULTS

To study changes in the local environment of the carboxyl terminus of γ_{PDE}, we engineered a mutant γ_{PDE} with a single cysteine at position 84 and introduced a fluorescence reporter group by chemical modification. Residue 84 was chosen because it was close to the carboxyl terminus but was thought not to be critical to the function of the carboxyl terminus in inhibiting α,β_{PDE} (*9*). The mutant was expressed as a T7 fusion protein with a 13 residue amino terminal tag, which results in a lower mobility of the unlabeled mutant protein relative to wild-type (WT) γ_{PDE} on SDS−PAGE (Figure 1B, lane C). To be able to label the γ_{PDE} subunit with a 1:1 stoichiometry at sulfhydryl sites, the single endogenous cysteine residue (at position 68) was mutated to a serine, as shown in Figure 1A. The IAF-labeled γ_{PDE} species were purified from both free probe and unlabeled protein using SDS−PAGE. IAF-labeled γ_{PDE} exhibits a lower mobility relative to the unlabeled species (*19*). Figure 1B shows the electrophoretic mobilities of wild-type (WT) γ_{PDE}, the IAF-labeled wild-type γ_{PDE} (designated F-WT γ_{PDE}), the C68S, Y84C γ_{PDE} mutant, and the IAF-labeled mutant (F-C68S, Y84C γ_{PDE}). Similar to the behavior of F-WT γ_{PDE}, the electrophoretic mobility of F-C68S, Y84C γ_{PDE} is retarded relative to the unlabeled C68S, Y84C γ_{PDE}. Isolating the fluorescent proteins from the SDS−PAGE gels helped to ensure that the IAF-labeled γ_{PDE} samples used in these studies were not contaminated with unlabeled γ_{PDE} and that the stoichiometry of the labeled subunit was 1:1.

Comparison of the Binding of Wild-Type γ_{PDE} and the C68S, Y84C γ_{PDE} Mutant to α,βPDE. The first indication that the C68S, Y84C γ_{PDE} mutant might provide new information regarding the γ_{PDE} -binding sites on the α,β_{PDE} subunits came when comparing its binding and inhibitory capabilities with those of the wild-type γ_{PDE}. Figure 2A,B represent two different readouts for the interactions of wild-type γ_{PDE} with the α,β_{PDE} subunits generated by trypsin treatment of holo-PDE. Previous studies have documented that trypsin treatment yields a constitutively active PDE molecule (tPDE) that contains the α and β_{PDE} subunits but lacks the γ_{PDE} subunits (*4*). The first readout (Figure 2A) shows the results obtained from fluorescence anisotropy measurements with IAF-labeled wild-type γ_{PDE} (F-WT γ_{PDE}). The anisotropy change represents a direct measure of the fraction of F-γ_{PDE} that is bound to the significantly larger α,β_{PDE} subunits (*9*, *22*). The best fit to the titration data shown in Figure 2A (solid line) yielded two F-WT γ_{PDE} molecules bound per α,βPDE dimer [consistent with a number of reports (e.g. refs *3*, *18*, *27*, and *28*)] with an apparent K_D value of 1.33 nM ± 0.47 nM (SE, $n = 3$).

Figure 2B shows a second readout for γ_{PDE} interactions with the α,β_{PDE} subunits (i.e. tPDE) which takes advantage of the well-documented finding that the addition of exogenous γ_{PDE} to tPDE inhibits its activity and restores the trypsin-treated enzyme to its basal state (*4*). The F-WT γ_{PDE} inhibited tPDE with a K_I value of approximately 2 nM. The good agreement between the K_D value and the apparent K_D value estimated from the fluorescence anisotropy measurements indicates that F-WT γ_{PDE} binding and inhibition can be described by a single class of binding sites, which is in agreement with the results from a number of previous studies (*4*, *5*, *18*, *28*).

However, a different outcome was obtained when the same experiments were performed using the C68S, Y84C γ_{PDE} mutant. Figure 2C shows that the purified F-C68S, Y84C γ_{PDE} subunit binds with high affinity to tPDE. The best fit to the fluorescence anisotropy data indicated a single high affinity γ_{PDE} binding interaction with the α,β_{PDE} dimer with an apparent K_D value of 53 pM ± 19 pM (SE, $n = 3$). Given that the apparent K_D value is 2 orders of magnitude lower than the protein concentrations that were necessary for making the anisotropy measurements, this value represents a lower bound estimate. Nonetheless, the data clearly indicate that the mutant γ_{PDE} species is capable of a high-affinity interaction with tPDE. This is noteworthy because the results from tPDE activity measurements suggest that the C68S, Y84C γ_{PDE} mutant is capable of only weakly inhibiting the enzyme activity (Figure 2D). The best fit to the data in Figure 2D yields a K_I value of 163 nM, which indicates a significantly weaker binding than the K_I value measured for the wild-type γ_{PDE} subunit (Figure 2B). The marked differences in the K_D and K_I values determined for the C68S, Y84C γ_{PDE} mutant sharply contrast what we observed for the wild-type γ_{PDE} species and provided us with an initial indication that the high-affinity binding site for the mutant γ_{PDE} may be distinct from the site which mediates inhibition of tPDE activity.

Competition by C68S, Y84C γ_{PDE} for WT γ_{PDE} Binding Sites, Kinetic Analyses, and Equilibrium Binding Studies. We next performed real-time competition experiments to obtain kinetic information for the binding of the WT and mutant γ_{PDE} molecules. Using fluorescence anisotropy, we first investigated the ability of unlabeled WT γ_{PDE} to exchange with the F-WT γ_{PDE} bound to tPDE. As would be expected for a simple competitive binding interaction, an excess of unlabeled WT γ_{PDE} was able to fully reverse the binding of F-WT γ_{PDE} to tPDE (Figure 3, left trace). The apparent k_{off} obtained from a single-exponential fit of these data yielded a rate constant of 0.0039 s^{-1} for F-WT γ_{PDE}. This rate is in reasonable agreement with the τ_{off} measured by Brown (*9*) in a previous report.

The right trace in Figure 3 shows the ability of *N*-ethylmaleimide (NEM)-labeled C68S, Y84C γ_{PDE} to compete with bound F-WT γ_{PDE}. In this case, we chose to use the NEM-C68S, Y84C γ_{PDE} mutant because it possessed a relatively weak binding ($K_I = 51$ nM), similar to that for F-C68S, Y84C γ_{PDE}, without interfering with the fluorescence measurements. When using a 20-fold excess of the NEM-labeled mutant, sufficient to saturate the C68S, Y84C γ_{PDE} binding site, only a 50% inhibition of the binding by F-WT γ_{PDE} was observed [49.5% ± 1.8% (SE, $n = 3$)]. The apparent k_{off} for F-WT γ_{PDE} upon the addition of the excess NEM-C68S, Y84C γ_{PDE} was 0.0034 s^{-1}. The subsequent addition of a 10-fold excess of unlabeled WT γ_{PDE} was able to compete with the remaining 50% of the F-WT γ_{PDE} bound to tPDE. The apparent k_{off} for the dissociation of this remaining pool of bound F-WT γ_{PDE} was 0.0023 s^{-1}. Control experiments demonstrated that unlabeled WT γ_{PDE} was able

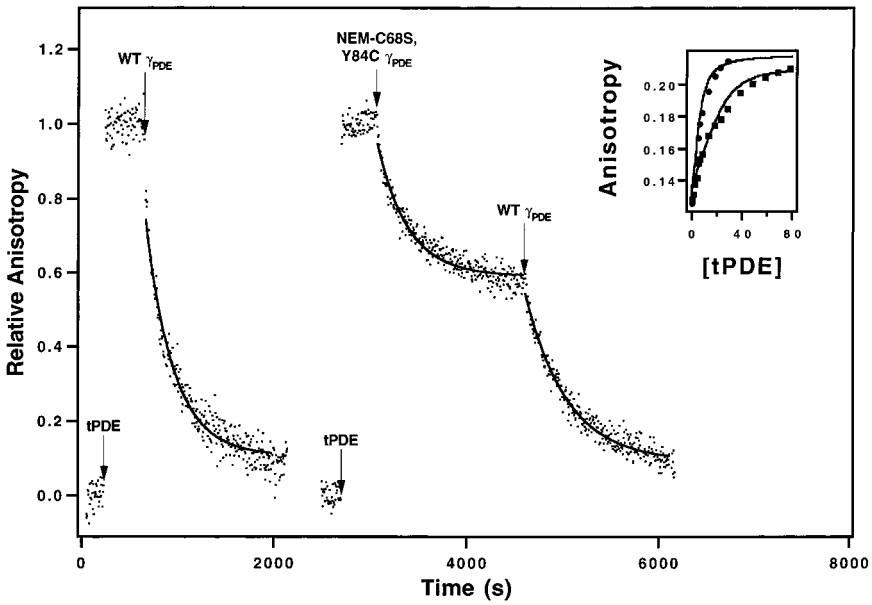

FIGURE 3: Competition between F-WT γ_{PDE} and NEM-C68S, Y84C γ_{PDE}. Each trace shows the fluorescence anisotropy of F-WT γ_{PDE}. F-WT γ_{PDE} was incubated with tPDE resulting in an increase in the fluorescence anisotropy. The subsequent addition of an excess of unlabeled γ_{PDE} resulted in the release of the F-WT γ_{PDE} from the tPDE as shown. The anisotropy trace on the left shows the dissociation of F-WT γ_{PDE} from tPDE upon the addition of unlabeled WT γPDE (0.4 μM, final concentration). The solid line indicates the best fit to a single time constant (k_{off} is 0.0039 s^{-1}). The anisotropy trace on the right shows the dissociation of F-WT γ_{PDE} upon the addition of NEM-C68S, Y84C γ_{PDE} (0.36 μM), followed by the dissociation of F-WT γ_{PDE} after making the same sample 0.4 μM in unlabeled WT γ_{PDE}. The k_{off} for F-WT γ_{PDE} upon the addition of NEM-C68S, Y84C γ_{PDE} is 0.0034 s^{-1}, with 49.5% $\pm$ 1.8% (SE, $n = 3$) of the F-WT γ_{PDE} dissociating from the tPDE after the addition of the NEM-C68S, Y84C γ_{PDE}. The subsequent addition of unlabeled WT γ_{PDE} results in the dissociation of the remaining 50% of F-WT γ_{PDE}, with the apparent k_{off} for this dissociation is 0.0023 s^{-1} (indicated by the solid line). Inset: Titration of F-WT γPDE (13.5 nM) with tPDE, alone (circles) or tPDE pretreated with a 4-fold excess of NEM-C68S, Y84C γPDE (squares), as monitored by changes in fluorescence anisotropy. The titrations were performed by adding aliquots from stock tPDE solutions (1 μM) to give the indicated nanomolar concentrations. The least-squares fit to the data (see Experimental Procedures) was obtained using a K_d of 1.4 nM and yielded a 2.16-fold reduction in the number of binding sites on tPDE (from 2 to 0.93) due to the pretreatment with NEM-C68S, Y84C γPDE.

to fully reverse the binding of the F-C68S, Y84C γ_{PDE} mutant and that the unlabeled C68S, Y84C γ_{PDE} was able to fully reverse the binding of F-C68S, Y84C γ_{PDE} (data not shown). Thus, the C68S, Y84C γ_{PDE} mutant effectively competes for a fraction (approximately half) of the WT γ_{PDE} binding sites with kinetics that, as expected, are limited by a dissociation time of characteristic WT γ_{PDE}.

The addition of an 100-fold excess of NEM-C68S, Y84C γ_{PDE} to the F-WT γ_{PDE}/tPDE complex (excess relative to F-WT γ_{PDE}) does approach a full reversal of the binding of F-WT (data not shown). Given the measured K_I for NEM-C68S, Y84C γ_{PDE} of 51 nM, this finding is consistent with the model that there is one site on α,β_{PDE} which binds C68S, Y84C γ_{PDE} mutants with high affinity (<1 nM) and one site on tPDE which binds C68S, Y84C γ_{PDE} with significantly lower affinity (>50 nM).

The inset to Figure 3 compares the binding of the F-WT γPDE to tPDE, alone, and to tPDE pretreated with the NEM-modified C68S, Y84C γPDE mutant, as monitored by changes in fluorescence anisotropy. The circles represent the binding of the F-WT γPDE to tPDE and the fit yields a K_D value of 1.4 nM. The squares show the binding of F-WT γPDE to tPDE that had been first treated with a 4-fold molar excess of NEM-C68S, Y84C γPDE. We fit the data using a function that contained an adjustable parameter (n) to take into account differences in the relative number of binding sites for F-WT γPDE (Experimental Procedures), due to the pretreatment of the tPDE with the NEM-C68S, Y84C mutant. Holding the value for the K_D describing the interactions between F-WT γPDE and tPDE at 1.4 nM, a least-squares fit to the data yielded an approximately 50% reduction in the number of total F-WT γPDE binding sites on tPDE when NEM-C68S, Y84C was present (from 2 sites per tPDE to 0.93 sites per tPDE). This then provides complementary evidence to the kinetic data which indicates that the labeled C86S,Y84C mutant effectively competes with WT γPDE at only one of the two binding sites on PDE.

Competition by C68S, Y84C γ_{PDE} for WT γ_{PDE} Inhibitory Sites, Enzymatic Activity. Perhaps the simplest model for explaining why the F-C68S, Y84C γ_{PDE} inhibits tPDE poorly at concentrations of the mutant protein which should be sufficient to saturate its high affinity binding site (Figure 2C,D) is that F-C68S, Y84C γ_{PDE} selectively binds with high affinity to a site that confers no inhibition of cGMP hydrolysis. In this case, the prebound F-C68S, Y84C γ_{PDE} would not prevent WT γ_{PDE} from inhibiting cGMP hydrolysis, because inhibition would be conveyed by the binding of WT γ_{PDE} to a distinct site.

To examine this possibility, the apparent K_I values for the inhibition of cGMP hydrolysis by F-WT γ_{PDE} were measured in the presence and absence of saturating concentrations of F-C68S, Y84C γ_{PDE} using the pH microelectrode assay. As shown in Figure 4, an excess of F-C68S, Y84C did not compete with the ability of F-WT γ_{PDE} to inhibit tPDE, but, on the contrary, increased the efficacy of F-WT γ_{PDE} in inhibiting cGMP hydrolysis. This is fully consistent with a model in which the high-affinity binding site for F-C68S, Y84C γ_{PDE} is not the site that mediates the inhibition of tPDE-catalyzed cGMP hydrolysis. Rather, we would propose that one site binds F-WT γ_{PDE} and conveys the inhibitory

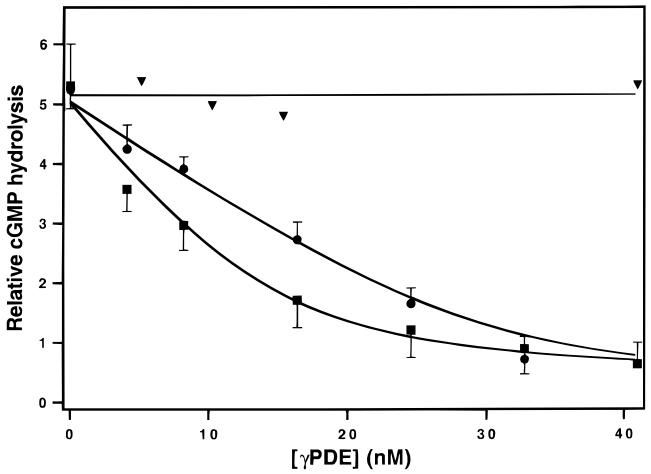

FIGURE 4: Effect of F-C68S, Y84C γ_{PDE} on the inhibition of tPDE by F-WT γ_{PDE}. The rate of cGMP hydrolysis of tPDE was measured using the pH microelectrode assay. A 3 pmol (15 nM) amount of tPDE was incubated with successive additions of γ_{PDE}. The closed triangles show the inability of F-C68S, Y84C γ_{PDE} to inhibit the activity of trypsin-treated PDE at these concentrations (the data are shown with a linear fit). The addition of F-WT γ_{PDE} to tPDE (shown as circles) resulted in an inhibition of the tPDE activity. The fit shows an apparent K_I of 2.0 nM and two F-WT γ_{PDE} binding sites per tPDE molecule. The addition of F-WT γ_{PDE} to 3 pmol (15 nM) tPDE in the presence of 9 pmol (45 nM) of F-C68S, Y84C γ_{PDE} is shown by the squares. The fit shows an apparent K_I of 2.3 nM, with a single F-WT γ_{PDE} binding site per tPDE molecule. The data shown are representative of 3 experiments.

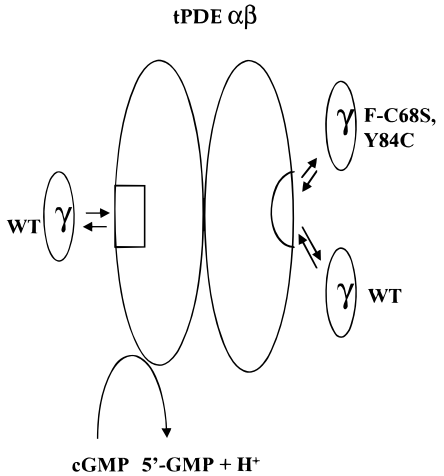

FIGURE 5: Schematic diagram of γ_{PDE} interacting with tPDE. This model depicts two binding sites for γ_{PDE} on tPDE, only one of which regulates PDE catalytic activity. Wild-type γ_{PDE} shows a similar affinity for either site. The F-C68S, Y84C γ_{PDE}, however, selectively binds to the noncatalytic site with high affinity.

activity of γ_{PDE}. The second site has a high affinity for both F-WT γ_{PDE} and F-C68S, Y84C γ_{PDE} but results in little or no change in cGMP hydrolytic activity (Figure 5). In this model, the F-C68S, Y84C γ_{PDE} would selectively bind to one of the two potential binding sites for WT γ_{PDE}. This would effectively result in an apparent increase in the concentration of WT γ_{PDE} and would cause an accompanying increase in the potency of WT γ_{PDE} to inhibit tPDE (Figure 4). The fit to the *lower curve* in Figure 4 shows that, in the presence of a 2-fold excess of F-C68S, Y84C γ_{PDE} (a concentration sufficient to saturate the high-affinity binding site for F-C68S, Y84C γ_{PDE}; see Figure 2C), the inhibition of tPDE by WT γ_{PDE} can be well-fitted assuming a single binding site per tPDE molecule. The apparent K_I for the WT γ_{PDE} in the presence of F-C68S, Y84C γ_{PDE} is 2.3 nM, in reasonable agreement with both the K_D value of 1.3 nM measured for the binding of F-WT γ_{PDE} to tPDE and the K_I value of 2.0 nM measured for the inhibition of tPDE by WT γ_{PDE} in the absence of F-C68S, Y84C γ_{PDE}. Therefore, the observed effect of saturating the high-affinity binding site for the γ_{PDE} mutant is to increase the effective concentration of F-WT γ_{PDE} as it pertains to the inhibition of PDE-mediated cGMP hydrolysis.

DISCUSSION

In the present study, we originally set out to probe the conformational changes within the carboxyl terminus of γ_{PDE} which are induced by binding to α,β_{PDE}. However, a careful characterization of the binding and functional properties of the F-C68S, Y84C γ_{PDE} led to some initially unforeseen results; the mutation (followed by IAF-modification of C84) appeared to result in a high-affinity binding interaction between the C68S, Y84C γ_{PDE} and the α,β_{PDE} heterodimer but a low potency inhibition of tPDE activity, such that the K_I value differed from the K_d value by nearly 2 orders of magnitude. Competition studies showed that at low concentrations (i.e. 10 nM), NEM-C68S, Y84C γ_{PDE} competed for only one of the two sites for WT γ_{PDE} on tPDE and PDE activity assays demonstrated that tPDE can be occupied with F-C68S, Y84C γ_{PDE} at its high-affinity binding sites and still be fully inhibited by WT γ_{PDE}. Taken together, these results are consistent with a model of two γ_{PDE} binding sites per α,β_{PDE} heterodimer. One confers the inhibitory properties, and the second, which binds F-C68S, Y84C γ_{PDE} with high affinity, plays as an of yet unknown function (Figure 5). The increase in the inhibitory potency of F-WT γ_{PDE}, when assayed in the presence of F-C68S, Y84C γ_{PDE}, is predicted by the model shown in Figure 5 since, under these conditions, the WT γ_{PDE} would exclusively bind to the inhibitory γ_{PDE} site (rather than binding to either the inhibitory site or to the noninhibitory site without preference).

An initial basis for differences in the binding of the two γ_{PDE} subunits to tPDE was proposed by Oppert et al. (*29*). Using peptides of α_{PDE} to compete for γ_{PDE} binding, they concluded that the amino terminus of the α_{PDE} monomer represented a critical region for γ_{PDE} binding. Given the relatively divergent sequence between the amino termini of α_{PDE} and β_{PDE} (36% identity over the first 100 amino acids, versus 72% identity for the entire sequence of 853 residues; *30*) and the proposed binding of γ_{PDE} to the amino terminal region of α_{PDE}, it was suggested that the two γ_{PDE} subunits might bind to the α,β_{PDE} subunits in a nonidentical fashion. However, more recent work by Artemyev et al. (*11*) has suggested that the amino termini of α_{PDE} and β_{PDE} are not important in the binding of γ_{PDE}. Proteolysis of PDE with trypsin causes the selective removal of the N-terminal domain of β_{PDE}, and this treatment does not cause large differences in the binding of the two γ_{PDE} subunits (*6*, *11*). They further showed with chemical cross-linking that the C-terminal inhibitory domain of γ_{PDE} binds to the carboxyl terminus of α_{PDE}, with a region (residues 751−763) that is relatively invariant between rod cell α_{PDE}, β_{PDE}, and cone PDE. Using peptides, Natochin and Artemyev (*10*) showed that the polybasic region of γ_{PDE} binds to sequences in α_{PDE} between residues 461 and 543. This region is also far from the N-terminal domain identified by Oppert et al. (*29*) and is also relatively invariant between PDE catalytic subunits.

Although primary sequence homology provides an argument for similarities in the function of the α and β subunits, this does not preclude the possibility that single amino acid differences which exist between α_{PDE} and β_{PDE} may alter the binding of γ_{PDE}. Similarly, cooperativity and/or differential binding of γ_{PDE} to each of the two sites on rod PDE also remains an open question (*4*, *6*, *27*, *33*). Along these lines, it is interesting to note that while the postulated γ_{PDE} binding site on the α_{PDE} subunit is in the immediate vicinity of the NKAD motif (*11*) that is thought to be involved in binding the cGMP guanine ring [thus providing a possible mechanism for γ_{PDE}-mediated inhibition by competition with substrate cGMP binding (*12*)], the corresponding sequence in β_{PDE} is NKAA. The aspartic acid residue within the NKXD motif, which is present in α_{PDE} but missing in β_{PDE}, is conserved in all GTP-binding proteins and is felt to be essential for the proper binding of the guanine ring. This then raises a number of important issues regarding whether in fact the α_{PDE} and β_{PDE} subunits are capable of equivalent cGMP binding and enzymatic activity and/or if the binding of γ_{PDE} to the β_{PDE} subunit would be expected to influence enzyme activity.

Other investigators have purified retinal PDE with only a single γ_{PDE} subunit (instead of two) bound per α,β_{PDE} heterodimer and have shown that this $\alpha,\beta,\gamma_{PDE}$ complex has approximately 50% of the activity measured for the α,β_{PDE} complex (*3*, *31*). Assuming that the single γ_{PDE} binds randomly to its two binding sites on α,β_{PDE}, these findings can be reconciled with our work suggesting that one WT γ_{PDE} site on α,β_{PDE} has inhibitory potential and the second γ_{PDE} site does not have inhibitory activity. In addition, Bruckert et al. (*32*) have demonstrated that a single activated α_T subunit interaction with bovine PDE is sufficient for full stimulation of cGMP hydrolysis activity, further supporting the existence of heterogeneity in γ_{PDE} inhibitory binding sites. Thus, we conclude that F-C68S, Y84C γ_{PDE} binds with high affinity (K_D < 1 nM) to a noninhibitory site. The inhibitory activity of the F-C68S, Y84C γ_{PDE} mutant at high concentrations is presumably due to the weaker binding to the second γ_{PDE} binding site on tPDE and this is reflected in the lower K_D for the binding of F-C68S, Y84C γ_{PDE} to the inhibitory site (K_I = 163 nM).

Thus, in summary, we would propose that there are preexisting differences in the two γ_{PDE} binding sites on the α,β_{PDE} subunits that are not apparent when monitoring the binding of WT γ_{PDE} but which are highlighted when examining the binding of the labeled C68S, Y84C γ_{PDE} mutant. The functional and physiological consequences of these differences remain to be determined. However, the potential differences in γ_{PDE} binding to α,β_{PDE} may underlie a more complicated regulation of the PDE compared to other G protein target/effector molecules which are thought to contain only a single G protein-binding site. In this regard, it has always been somewhat puzzling that the amount of activated α_T subunit needed to maximally stimulate PDE activity typically far exceeds the apparent K_D (~10 nM) for high-affinity α_TGTPγS/γ_{PDE} interactions and that previous studies have indicated some form of cooperativity in the stimulatory interactions of two α_T subunits with a single holo-PDE molecule (*17*). Future studies will focus on further examining the ability of α_TGTPγS to differentially interact with the two γ_{PDE} subunits on the PDE molecule and on the potential cooperativity between the two γ_{PDE} binding sites.

REFERENCES

1. Stryer, L. (1986). Cyclic GMP Cascade of Vision. *Annu. Rev. Neurosci. 9*, 87−119.
2. Chabre, M. D., and Deterre, P. (1989). Molecular Mechanism of Visual Transduction. *Eur. J. Biochem. 179*, 225−266.
3. Deterre, P., Bigay, J., Forquet, F., Robert, M., and Chabre, M. (1988). *Proc. Natl. Acad. Sci. U.S.A. 85*, 2424−2428.
4. Wensel, T. G., and Stryer, L. (1990) *Biochemistry 29*, 2155−2161.
5. Otto-Bruc, A., Antonny, B., Vuong, T. M., Chardin, P., and Chabre, M. (1993) *Biochemistry 32*, 8636−8645.
6. Artemyev, N. O., and Hamm, H. E. (1992). *Biochem. J. 283*, 273−279.
7. Artemyev, N. O., Skiba, N. P., Mills, J. S., and Hamm, H. E. (1993). *Methods Comput. Methods Enzymol. 5*, 220−228.
8. Lipkin, B. M., Dumler, I. L., Muradov, K. G., Artemyev, N. O., and Etingof, R. N. (1988). *FEBS Lett. 234*, 287−290.
9. Brown, R. L. (1992) *Biochemistry 31*, 5918−5925.
10. Natochin, M., and Artemyev, N. O. (1996). *J. Biol. Chem. 271*, 19964−19969.
11. Artemyev, N. O., Natochin, M., Busman, M., Schey, K. L., and Hamm, H. E. (1996). *Proc. Natl. Acad. Sci. U.S.A.. 93*, 5407−5412.
12. Granovsky, A., Natochin, M., and Artemyev, N. O. (1997). *J. Biol. Chem. 272*, 11686−11689.
13. Yamazaki, A., Bartucca, F., Ting, A., and Bitensky, M. W. (1982). *Proc. Natl. Acad. Sci. U.S.A. 72*, 3702−3706.
14. Gillespie, P. G., and Beavo, J. A. (1989). *Proc. Natl. Acad. Sci. U.S.A. 86*, 4311−4315.
15. Arshavsky, V. Y., Dumke, C. L., and Bownds, M. D. (1992). *J. Biol. Chem. 267*, 24501−24507.
16. Cote, R. H., Bownds, M. D., and Arshavsky, V. Y. (1994). *Proc. Natl. Acad. Sci. U.S.A. 91*, 4845−4849.
17. Phillips, W. J., Trukawinski, S., and Cerione, R. A. (1989). *J. Biol. Chem. 264*, 16697−16688.
18. Erickson, J. W., and Cerione, R. A. (1991) *Biochemistry 30*, 7112−7118.
19. Erickson, J. W., Mittal, R., and Cerione, R. A. (1995) *Biochemistry 34*, 8693−8700.
20. Brown, R. L., and Stryer, L. (1989) *Proc. Natl. Acad. Sci. U.S.A. 86*, 4922−4926.
21. Skiba, N. P., Artemyev, N. O., and Hamm, H. E. (1995) *J. Biol. Chem. 270*, 13210−13215.
22. Berger, A. L., Cerione, R. A., and Erickson, J. W. (1997). *J. Biol. Chem. 272*, 2714−2721.
23. Haugland, R. P. (1994). *Molecular Probes Handbook of Fluorescent Probes and Research Chemicals*, 5th ed. Molecular Probes, Inc., Eugene, OR.
24. Kroll, S., Phillips, W. J., and Cerione, R. A. (1989) *J. Biol. Chem. 264*, 4490−4497.
25. Gierschik, P., Simons, C., Woodard, C., Somers, R., and Spiegel, A. (1984) *FEBS Lett. 172*, 321−325.
26. Yee, R., and Liebman, P. A. (1978) *J. Biol. Chem. 253*, 8902−8909.
27. Whalen, M. W., and Bitensky, M. W. (1989). *Biochem. J. 259*, 13−19.
28. Erickson, J. W., and Cerione, R. A. (1993) *J. Biol. Chem. 268* (5), 3328−3333.
29. Oppert, B., Cunnick, J. M., Hurt, D., and Takemoto, D. J. (1991). *J. Biol. Chem. 266*, 16607−16613.
30. Lipkin, V. M., Khramtsov, N. V., Vasilevskaya, I. A., Atabekova, N. V., Muradov, K. G., Gubanov, V. V., Li, T., Johnston, J. P., Volpp, K. J., and Applebury, M. L. (1990). *J. Biol. Chem. 265*, 12955−12959.
31. Catty, P., Pfister, C., Bruckert, F., and Deterre, P. (1992). *J. Biol. Chem. 267*, 19489−19493.
32. Bruckert, F., Catty, P., Deterre, P., and Pfister, C. (1994). *Biochemistry 33*, 12625−12634.
33. Whalen, M. M., Bitensky, M. W., and Takemoto, D. J. (1990) *Biochem. J. 265*, 655−658.

BI981683M